Electronic Supplemental Information (ESI)

Synergetic effect of TiO_2/ZnO bilayer photoanodes realizing exceptionally high V_{OC} for dye-sensitized solar cells under outdoor and indoor illuminations

Anooja Jagadeesh,[a,b] Ganapathy Veerappan,[c] P. Sujatha Devi, [a,b] K. N. Narayanan Unni [a,b] and Suraj Soman* [a,b]

[a] Photosciences and Photonics Section, Chemical Sciences and Technology Division, CSIR-National Institute for Interdisciplinary Science and Technology (CSIR-NIIST), Thiruvananthapuram 695019, India.
[b] Academy of Scientific and Innovative Research (AcSIR), Ghaziabad-201002, India.
[c] Centre for Solar Energy Materials, International Advanced Research Centre for Powder Metallurgy and New Materials (ARCI), Balapur, Hyderabad 500005, Telangana, India

*Correspondence: suraj@niist.res.in

Supporting information includes:
Experimental section
Figures S1 to S12
Tables S1 to S5
References

Other Supplementary Material for this manuscript includes:
Supplementary Video S1
Supplementary Video S2

Experimental Section

Materials. All chemicals used for material synthesis and device fabrication were HPLC grade and used without further extraction or purification. Zinc nitrate hexahydrate ($Zn(NO_3)_2{\cdot}6H_2O$) and urea (CON_2H_4) used for microstructure synthesis, as well as ethyl cellulose and α-terpineol used for paste preparation, were purchased from Merck. The additives such as Bis(trifluoromethane)sulfonimide lithium salt (LiTFSI), 4-tert-Butylpyridine (TBP), ethylenedioxythiophene (EDOT) and sodium dodecyl sulphate (SDS) were also purchased from Merck. Ttitania paste (18NR-T) and blocking layer solution (BL) was procured from GreatcellSolar (Australia). Y123, MS5 dye and copper complexes, Bis(2,9-dimethyl-1,10-phenanthroline copper(I) bis(trifluoromethanesulfonyl)imide ($[Cu(dmp)_2]^{1+}$) and Bis(2,9-dimethyl-1,10-phenanthroline copper(II) bis(trifluoromethanesulfonyl)imide chloride ($[Cu(dmp)_2]^{2+}$), were purchased from Dyenamo A.B (Sweden). Fluorine doped SnO_2 (FTO) coated glasses, TEC10 used for photoanode preparation and TEC7 for counter electrode fabrication were purchased from Merck and GreatcellSolar. The thermoplastic used for assembling the device (surlyn) was also obtained from GreatcellSolar.

Synthesis and characterization of ZnO hierarchical structures. ZnO hierarchical structure synthesis was done following a simple procedure involving zinc nitrate hexahydrate and urea as the precursor and precipitant, respectively.[1] In the typical synthesis process, an aqueous solution of zinc nitrate hexahydrate was added dropwise into an aqueous urea solution with a specific concentration under constant and vigorous stirring.

Zinc nitrate hexahydrate ($Zn(NO_3)_2{\cdot}6H_2O$) dissolves in water to generate Zn^{2+} ions.[equation 4] At the same time, when urea is dissolved in water and heated above 60°C, it undergoes hydrolysis and decomposes to liberate carbonate (CO_3^{2-}) and hydroxyl (OH^-) ions [equation 5 and 6].[2]

$$Zn(NO_3)_2 \cdot 6H_2O + H_2O \rightarrow Zn^{2+} + 2NO_3^- + 7H_2O \quad (4)$$

$$CON_2H_4 + 3H_2O \rightarrow CO_2\,(g) + 2NH_3H_2O \quad (5)$$

$$2NH_3H_2O + CO_2 \rightarrow 2NH_4^+ + CO_3^{2-} + OH^- \quad (6)$$

The OH^- ions increase the pH of the reaction mixture to offer a favourable reaction condition in which Zn^{2+} ions react with the CO_3^{2-} and OH^- ions in the reaction mixture to form layered hydroxide zinc carbonate (LHZC, $Zn_5CO_3(OH)_6.H_2O$). [equation 7] LHZC, when annealed above 300°C will lose CO_2 and water to give pure ZnO [equation 8]. In our device fabrication procedure, we generally anneal the sample-coated electrodes at 500°C.

$$4Zn^{2+} + CO_3^{2-} + 6OH^- + H_2O \rightarrow Zn_4CO_3(OH)_6 \cdot H_2O \quad (7)$$

$$Zn_4CO_3(OH)_6 \cdot H_2O \rightarrow 4ZnO + 4H_2O + CO_2 \quad (8)$$

In order to synthesize three different samples, three reaction mixtures were prepared with the same concentration of zinc nitrate hexahydrate (0.02 M) and three different concentrations of urea (0.03 M, 0.08 M and 0.8 M). The reaction mixtures were stirred at 1000 rpm for one hour, transferred to the furnace, and kept at 90°C for 24 hours. The white precipitates obtained were washed with DI water and ethanol before drying at 60°C for 8 hours. The as-synthesized samples, when annealed at 500°C gave ZnO.

The morphology of the as-synthesized samples was determined using the Scanning Electron Microscope (SEM), Zeiss EVO 18 cryo-SEM Special Ed, at an acceleration voltage of 15.0 kV. The specific surface area of these samples was calculated using the Brunauer-Emmett-Teller (BET) model from the data obtained by standard N_2 adsorption technique (using Tristar II, Micrometrics surface area analyser) after degassing at 200^{o}C for 2h. The morphological features, crystallite size and orientation of the annealed samples were further analysed using High-Resolution Transmission Electron Spectroscope, JEOL JEM F 200 EELS STEM and EDS. Particle size and crystallite size were estimated from the SEM and TEM micrographs using ImageJ software. The crystallinity and phase were confirmed using the X-ray diffraction patterns recorded by a Malvern PANalytical B.V. X-ray diffractometer in the 2θ range 20^o to 80^o with a slow scan mode. The crystal size and phase of the samples were determined by analysing the XRD patterns using X'pert Highscore software.

Photoanode preparation and characterization. Photoanodes for DSCs were prepared using FTO-coated glass (TEC 10) as the conducting substrate. The FTO substrates were cut into small pieces of required dimensions (1.6 cm x 1.6 cm) and cleaned systematically with a soap solution (for 30 minutes), de-ionized water (for 30 minutes), isopropanol (for 15 minutes) and acetone (for 15 minutes) in an ultrasonic bath, followed by annealing at 500^{o}C for 30 minutes. The cleaned FTO glasses were undergone UV/ozone treatment for 15 minutes prior to the deposition of the TiO_2 blocking layer by $TiCl_4$ treatment, in which the electrodes were immersed in 50 mM aqueous solution of $TiCl_4$ at 75^{o}C for 30 minutes. This was followed by a step-wise annealing process in which the $TiCl_4$ treated FTO substrates were heated at a slow rate and maintained at 150^{o}C for 10 minutes, 300^{o}C for 10 minutes, 350^{o}C for 10 minutes, 450^{o}C for 10 minutes and finally at 500^{o}C for 30 minutes, followed by slow cooling. The standard TiO_2 photoanode (T) was fabricated with a 6 µm thick mesoporous semiconducting layer of commercial titania paste (18NR-T) (device active area of 0.24 cm^2) via screen printing, whereas the ZnO based photoanodes (T+Z) were prepared by coating an additional layer of ZnO paste over the active layer, after drying the TiO_2 layer at 100^{o}C for 10 minutes. The as-synthesized powder samples were converted to paste by grinding in a mortar before and after adding a mixture of ethyl cellulose (10 wt%) and α-terpineol (60 wt%), which were heated at 100^{o}C. Finally, the electrodes were subjected to the step-wise annealing process, as mentioned above. In case of the electrodes utilizing blocking layers (BL), commercial TiO_2 BL solution was deposited over the T+Z photoanode via screen printing, prior to the annealing process.

The morphological and crystallographic studies of unsensitized photoanodes were carried out by FESEM (Zeiss Gemini 500), and X-ray diffraction patterns were recorded by a Malvern PANalytical B.V. X-ray diffractometer, in the 2θ range 20^o to 70^o. Mott Schottky analysis was conducted on the dummy cells fabricated with unsensitized photoanodes (detailed fabrication steps provided in the following section) using a Biologic electrochemical workstation (VMP3). UV-Visible spectrometer (Shimadzu model 2100) was used to carry out the dye loading studies as described below. A dye stock solution was prepared by dissolving 0.01 mM of the dye in a 1:1 mixture of acetonitrile and tert-butanol. The dye solution was divided into two equal portions (solution 1 and solution 2). The photoanode (FTO coated with the mesoporous TiO_2 or TiO_2/ZnO layer), the dye loading to be obtained, is immersed in solution 2. After 16 hrs of dye soaking, solution 2 is retrieved. The photoanode is then washed with 1 mL of acetonitrile to remove the weakly adsorbed dye which is also added to solution 2. To compensate for the variation in concentration, the same amount of acetonitrile is added to solution 1. Now, the UV-visible absorption spectra of both solutions are recorded and the maximum

absorbance is obtained as abs1 and abs2 for solutions 1 and 2, respectively. Finally, the amount of dye adsorbed per unit area (mol/cm^2) of the mesoporous layer is estimated as,

$$dye\ loading\ = \frac{(abs1 - abs2)V}{\varepsilon s l} \quad (9)$$

where V is the volume of the solution, ε is the molar extinction coefficient of the dye, s is the photoanode's active area, and l is the path length of the incident light in the solution.

Fabrication and characterization of DSCs. Devices were fabricated using our existing dye-sensitized solar cell/module semi-automated fabrication facility (Fig. S9). One batch consists of 12 devices, and 3 consecutive batches were done for each condition to calculate the error. For fabricating DSCs, the photoanodes prepared as mentioned in the previous section were sensitized with dye by immersing them in 0.1mM of the dye solution prepared in a 1:1 mixture of acetonitrile and tert-butanol for 16 hours. The conducting polymer viz. poly(3,4-ethylene dioxythiophene) (PEDOT) deposited on FTO (TEC7) substrate was utilized as the counter electrodes for our devices, the preparation of which is described below. The FTO substrates of dimensions 1.6 cm x 1.6 cm were cut and drilled with two holes prior to ultrasonic cleaning using soap solution (for 45 minutes), de-ionized water (for 45 minutes) and ethanol (for 45 minutes). The cleaned substrates were annealed at 500^{o}C for 30 minutes and cooled down to room temperature, followed by UV/ozone treatment for 15 minutes. A micellar aqueous solution of the monomer, EDOT (0.01M) and the surfactant, SDS (0.1M), was prepared. The predrilled and cleaned FTO substrate (to be used as CE) and a reference electrode (an FTO or metal substrate) were connected to an external current source (Metrohm Autolab workstation) and immersed in the above solution. Electro-polymerization is performed by passing a current of 13 mA for 1.5 seconds. The PEDOT film coated on the FTO substrates was allowed to air dry at room temperature. Subsequently, the dye-sensitized photoanode and the counter electrode were fused using a 25 µm thick thermoplastic spacer by hot pressing at 120^{o}C. Finally, the inter-electrode spacing was infused with the electrolyte solution via the holes in the counter electrode, which were then sealed to prevent solvent evaporation and leakage. The electrolyte was prepared by dissolving the copper dimethyl phenanthroline species (0.2 M $[Cu(dmp)_2]^{1+}$ and 0.04 M $[Cu(dmp)_2]^{2+}$) along with 0.1 M LiTFSI and 0.6 M TBP as additives in acetonitrile solvent.

Photovoltaic characterization of the fabricated DSCs was done under ambient conditions (25^{o}C and 50% humidity) using a source meter (Keithley) along with a class AAA solar simulator (Model PVIV-94043A, Newport) under one sun condition (100 mWcm^{-2}, AM 1.5G), with a scan rate of 100 mV/s. The light intensity was calibrated using a certified reference silicon solar cell and a power meter. The stability test was done by keeping the devices in dark under ambient condition (27°C room temperature and 80% humidity condition), and the measurements were done using the class AAA Newport solar simulator. J-V characterization under indoor light conditions was carried out using Dyenamo AE05 potentiostat, with warm white compact fluorescent lamp, CFL (Osram, 14W/2700K) and daylight emitting diode, LED (Osram, 4W/6500K) as a light source inside a custom-made indoor light measurement setup (Figure S9). A highly sensitive photodetector coupled with a UV-Vis-NIR spectrometer (Ocean optics, DH-2000-BAL) was used to measure the CFL and LED irradiance spectra and incident power density (Figure S10) and was cross verified using a certified irradiance measuring unit from Dyenamo AB (DN-AE06). The measurements were done for 500 lux and 1000 lux. A black

mask with a circular aperture of 0.11 cm^2 was used for J-V measurements under one sun, and a larger aperture of 0.34 cm^2 was used for indoor measurements. Incident photon-to-current conversion efficiency (IPCE) measurement was done using a 250 W Xenon lamp coupled with a monochromator. Electrochemical Impedance Spectroscopy (EIS), Open Circuit Voltage Decay (OCVD) and Intensity Modulated Photovoltage Spectroscopy (IMVS) measurements were carried out using the electrochemical workstation (Autolab, Metrohm). EIS was done under dark conditions, providing a bias voltage in the range 0.8V-1.1V, with a frequency ranging from 100mHz to 100kHz. The fitting of the plots was done using ZView software in order to obtain the various parameters such as chemical capacitance (C_μ), charge transfer resistance (R_{ct}), lifetime (τ_n) and transport time (τ_d). OCVD measurements were done by illuminating the cells using a white LED under open circuit conditions. IMVS measurements were done using the same workstation along with a LED driver and white LED by applying a frequency ranging from 1 Hz to 10kHz. Photocurrent and photovoltage decay measurements were done using the Dyenamo toolbox. Measurements were done using an LED source, and the modulation amplitude was always maintained at less than 10% of the steady-state value.

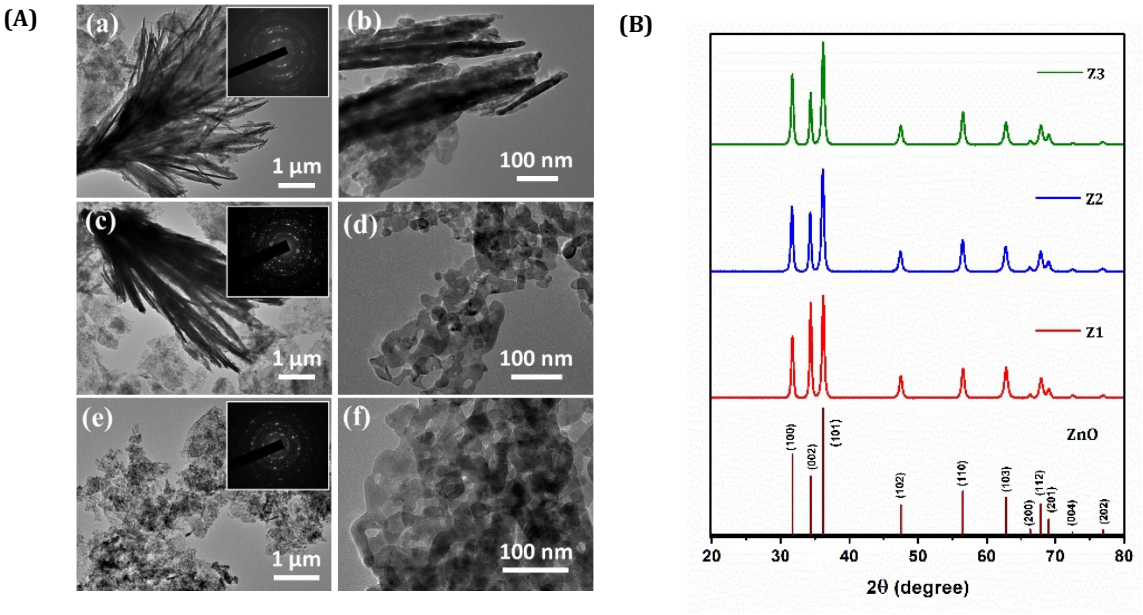

Fig. S1 (A) HRTEM images of annealed samples of (a,b) Mimosa flower-like microstructures (Z1); (c,d) Dandelion flower-like microstructures (Z2); (e,f) Rose flower-like microstructures (Z3). SAED patterns are provided in the inset. (B) XRD patterns of ZnO samples (Z1, Z2 and Z3) annealed at 500^{o}C.

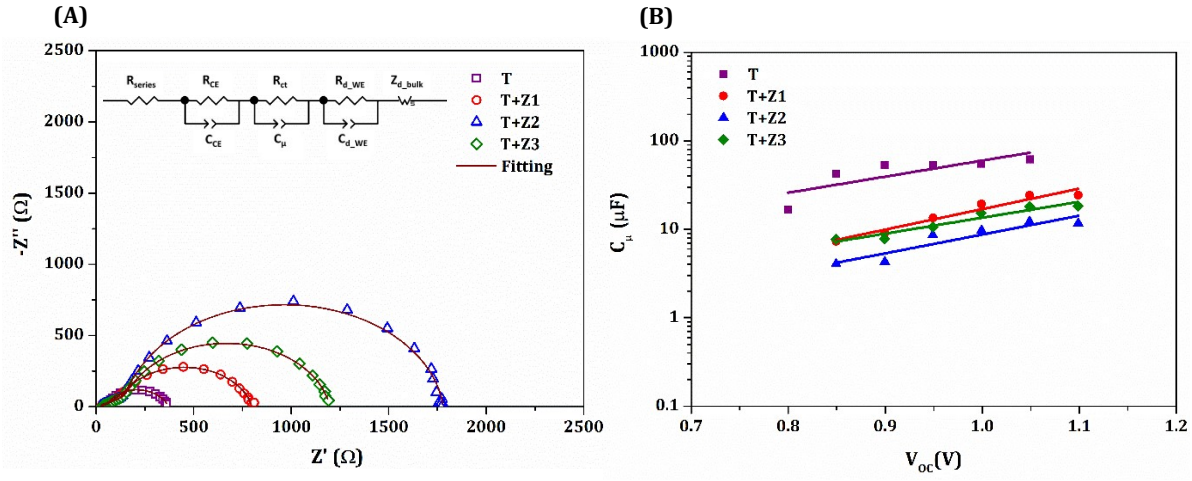

Fig. S2 (A) Nyquist plots of T, T+Z1, T+Z2 and T+Z3 devices fabricated using Y123 sensitizer and $[Cu(dmp)_2]^{1+/2+}$ redox electrolyte obtained from EIS measurement under dark condition (at a bias of 1V) along with the modified Randle's circuit used for fitting them, in which R_{series}, R_{CT} and R_{CE} symbolize the series resistance, charge transfer resistance at TiO_2/dye/electrolyte interface and counter electrode interface respectively, whereas C_μ and C_{CE} respectively specify the chemical capacitance and capacitance due to charge accumulation at the counter electrode/electrolyte interface. The Warburg diffusion element ($Z_{d\text{-}bulk}$) corresponds to resistance ($R_{d\text{-}bulk}$) for the diffusion of redox species in the bulk of the electrolyte, while $R_{d\text{-}WE}$ corresponds to the diffusion of charged species within the mesoporous semiconductor layer. (B) Chemical capacitance (C_μ), determined by fitting Nyquist plots, plotted against V_{OC}.

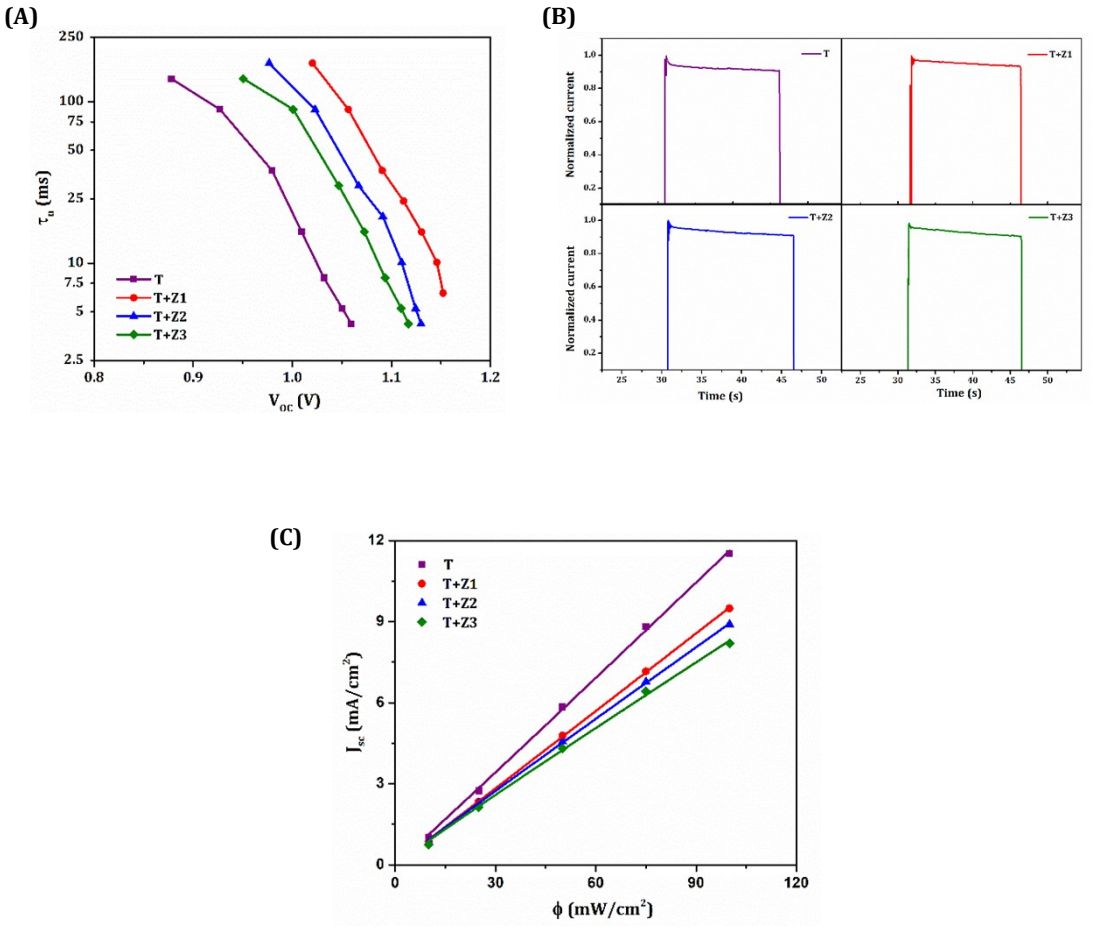

Fig. S3 (A) Lifetime as a function of V_{OC} obtained from IMVS, (B) current transients at an illumination intensity of 100 mW/cm^2 and (C) J_{SC} versus light intensity plot obtained for T, T+Z1, T+Z2 and T+Z3 DSCs, employing Y123 sensitizer and $[Cu(dmp)_2]^{1+/2+}$ redox electrolyte.

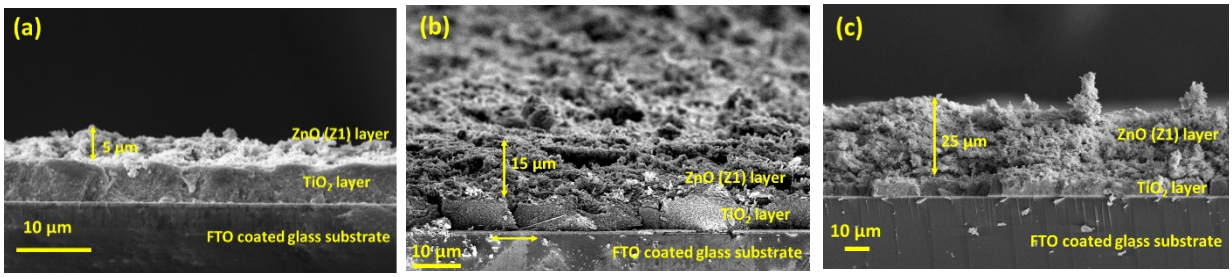

Fig. S4 Cross-sectional SEM images of T+Z1 photoanodes with different ZnO layer thicknesses, (a) 5µm, (b) 15µm and (c) 25µm.

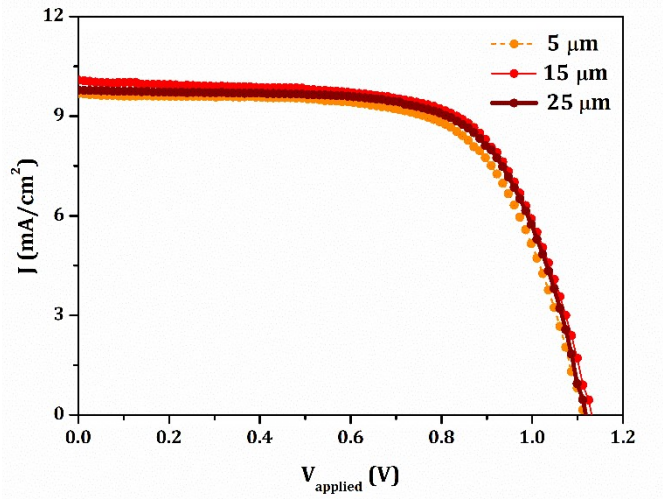

Fig. S5 J-V curves obtained under AM 1.5G solar irradiation (100 mW/cm^2) for T+Z1 devices with different ZnO layer thicknesses (5µm, 15µm and 25µm), sensitized using Y123 dye and $[Cu(dmp)_2]^{1+/2+}$ redox electrolyte.

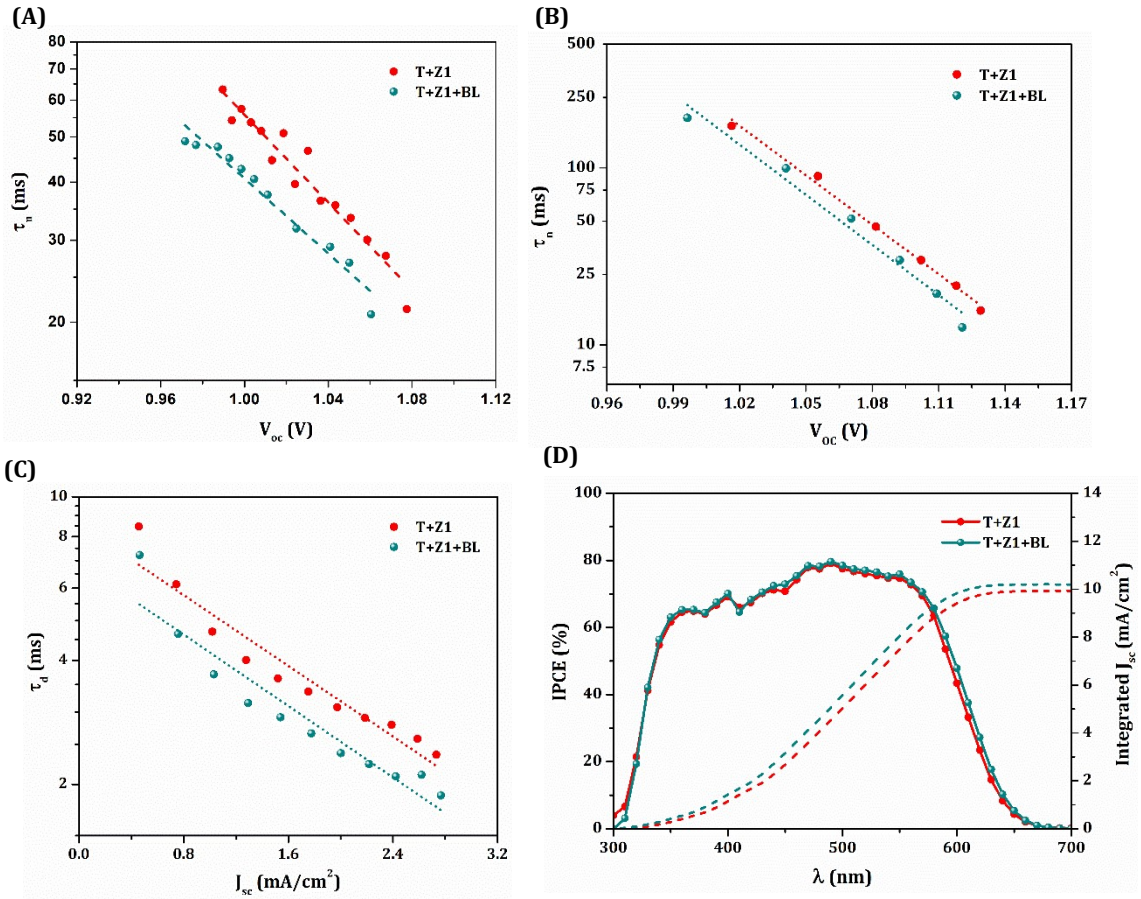

Fig. S6 Lifetime as a function of V_{OC} obtained from (A) OCVD and (B) IMVS measurements; (C) transport time as a function of J_{SC} obtained from transient photocurrent decay measurement and (D) IPCE

spectra and integrated J_{SC} plot (dotted line) for TiO_2/ZnO bilayer DSCs with blocking layer (T+Z1+BL) and without blocking layer (T+Z1), employing Y123 sensitizer and $[Cu(dmp)_2]^{1+/2+}$ redox electrolyte.

(A)

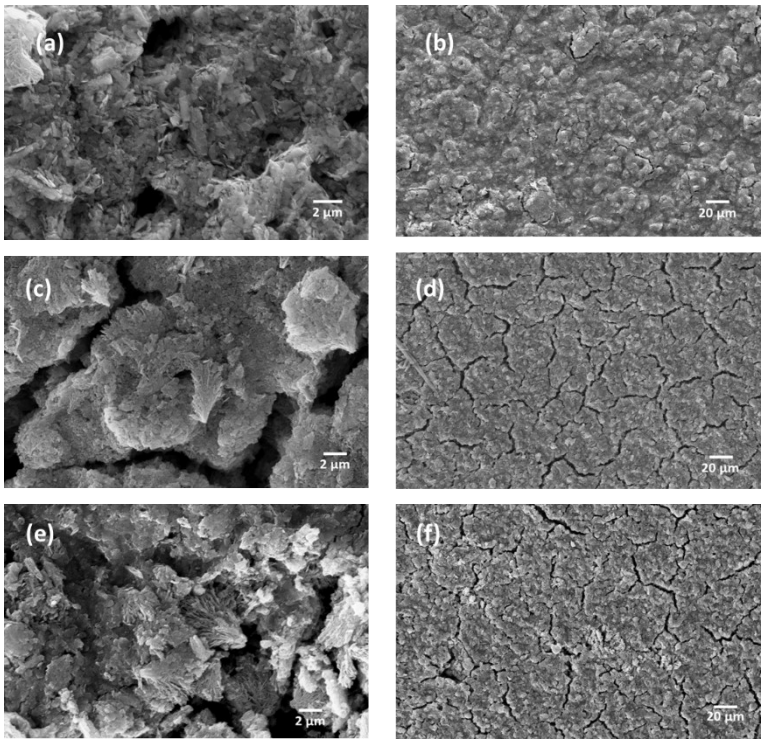

Fig. S7 (A) SEM images of (a,b) freshly prepared T+Z1 film (without dye adsorption and electrolyte exposure), (c,d) Y123 dye adsorbed T+Z1 films after 1000 h of electrolyte exposure, (e,f) Y123 dye adsorbed T+Z1+BL films after 1000 h of electrolyte exposure; (B) XRD patterns of Y123 dye adsorbed T+Z1 and T+Z1+BL films after 1000 h of electrolyte exposure.

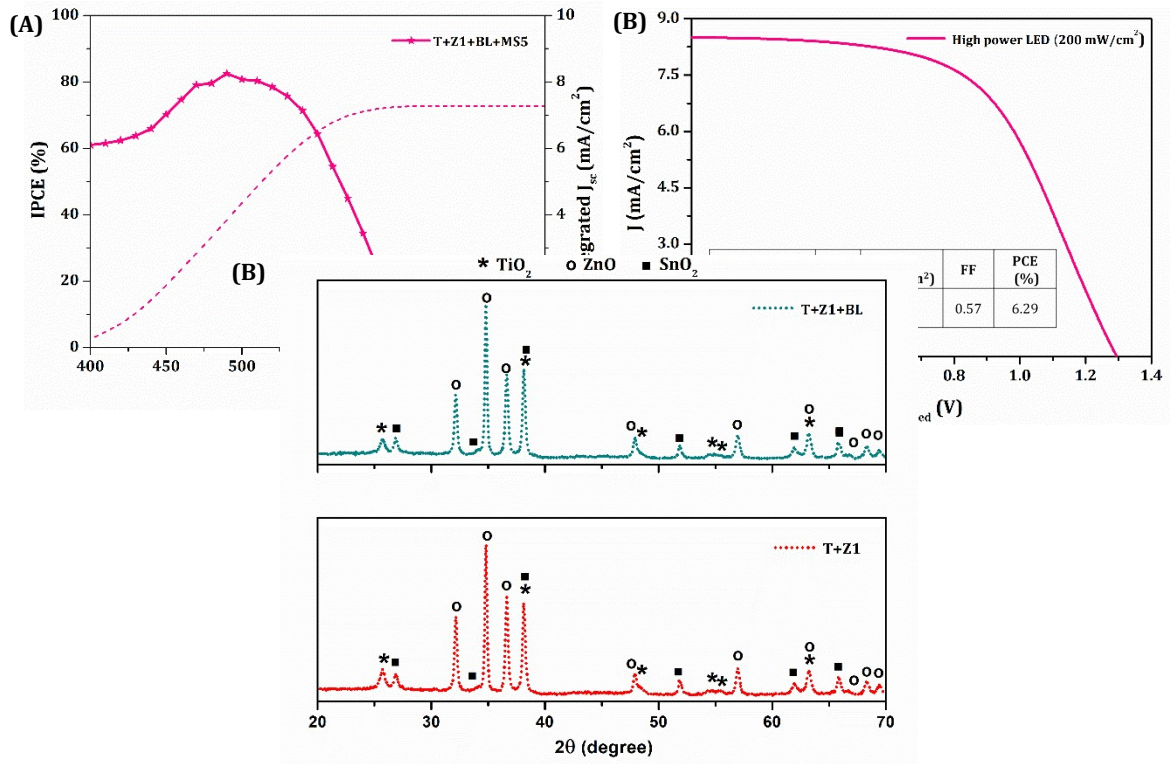

Fig. S8 (A) IPCE spectra corresponding to one sun illumination (100 mW/cm^2) with integrated J_{sc} plot (dotted line) and (B) J-V curves obtained (PV parameters provided in inset) under high power LED illumination (200 mW/cm^2) for T+Z1+BL devices employing MS5 dye and $[Cu(dmp)_2]^{1+/2+}$ redox electrolyte.

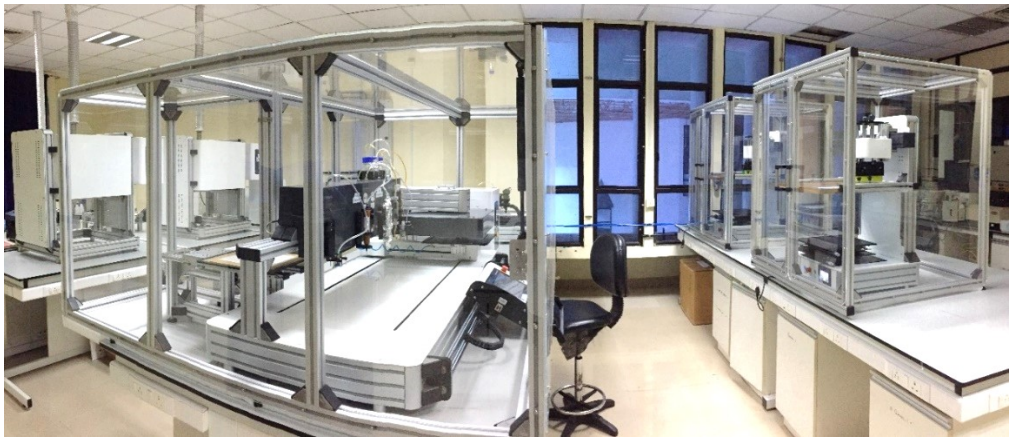

Fig. S9 Semi-automated dye-sensitised solar cell/module fabrication facility used to fabricate DSCs used in the present study.

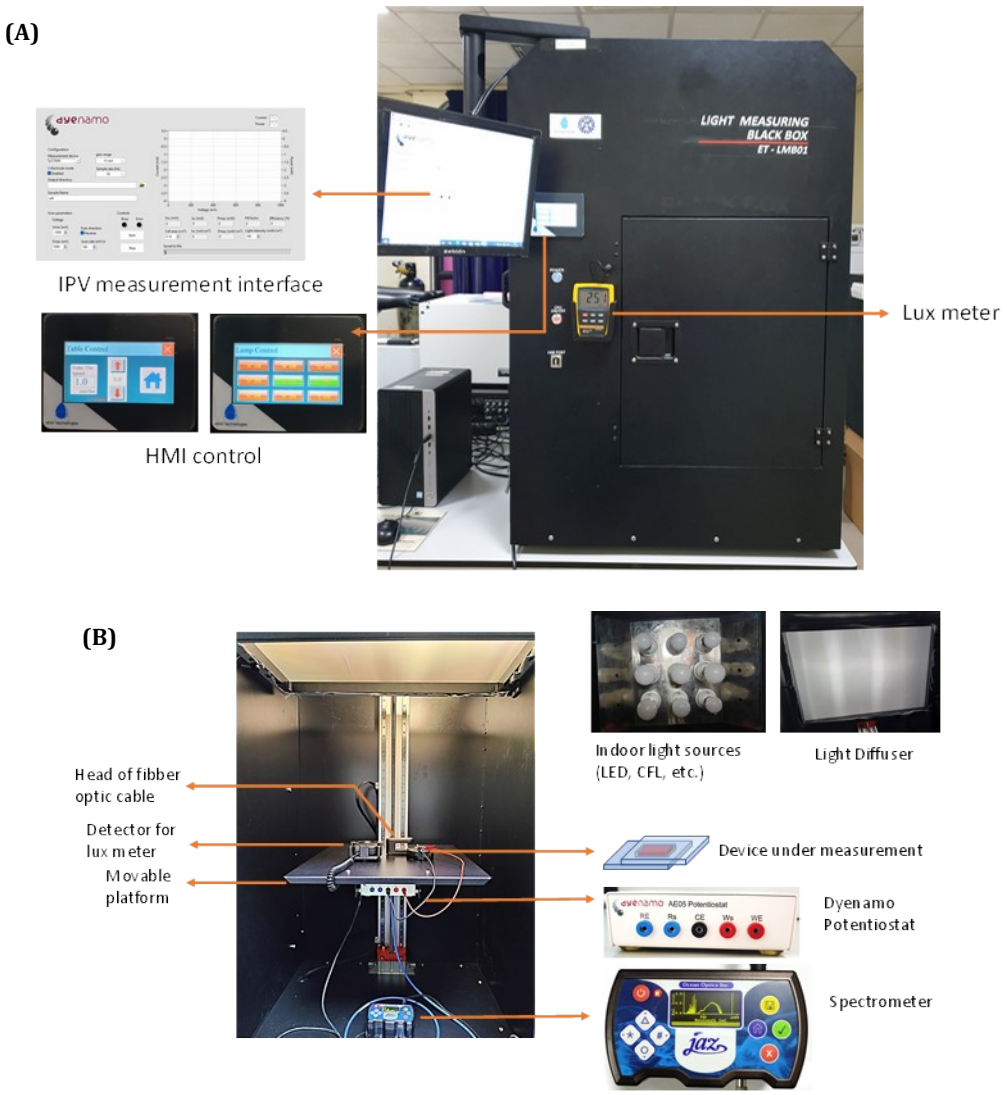

Fig. S10 (A) Outside view and (B) inside view of the custom-designed indoor photovoltaic measuring setup integrated with optical fibre spectrometer (Ocean optics, DH-2000-BAL), power meter (LX-101A) and potentiostat (Dyenamo AE05) used for carrying out the indoor photovoltaic measurements.

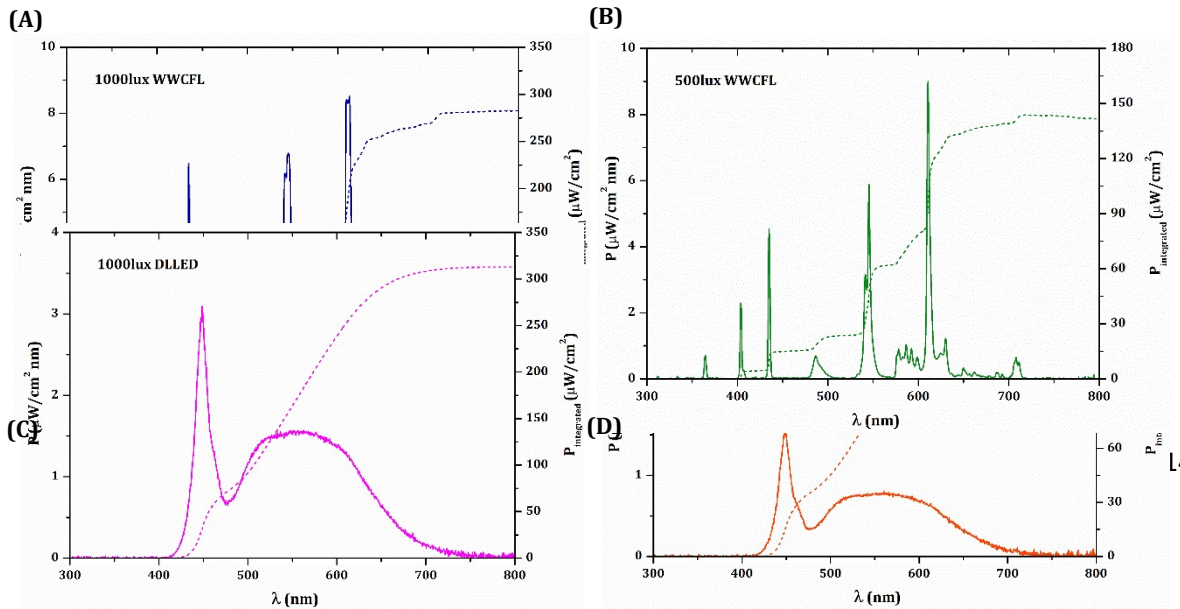

Fig. S11 Spectral irradiance and integrated power spectra under (A) 1000 lux and (B) 500 lux warm white (WW) CFL illumination, (C) 1000 lux and (D) 500 lux daylight (DL) LED illumination.

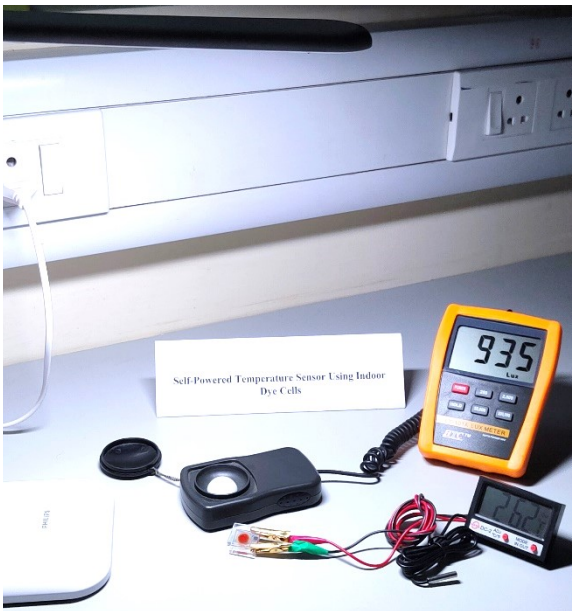

Fig. S12 A temperature sensor (ACETEQ DC-2) powered using a single TiO_2/ZnO bilayer DSC (active area 0.24 cm^2) fabricated using MS5 dye and $[Cu(dmp)_2]^{1+/2+}$ redox electrolyte under indoor LED reading lamp (935 lux LED light).

Table S1. Particle size, crystallite size and surface area obtained for the ZnO samples (Z1, Z2 and Z3).

ZnO sample	Average particle size from SEM (μm)	Average crystallite size from XRD (nm)	Average crystallite size from HRTEM (nm)	BET surface area (m^2/g)
Z1	11.49 ± 0.98	34.74 ± 3.29	33.94 ± 6.87	81.7
Z2	10.12 ± 1.27	35.53 ± 4.95	33.89 ± 1.49	58.3
Z3	9.58 ± 2.55	31.78 ± 4.46	32.96 ± 2.22	35.3

Table S2. Parameters obtained by fitting the corresponding Nyquist plots for T, T+Z1, T+Z2 and T+Z3 devices obtained from EIS carried out at a bias of 1V employing Y123 sensitizer and $[Cu(dmp)_2]^{1+/2+}$ redox electrolyte.

Parameters	T	T+Z1	T+Z2	T+Z3
R_{ct}	29.92 Ω	84.47 Ω	119.3 Ω	91.57 Ω
C_{μ}	55 µF	19.3 µF	9.69 µF	15.3 µF
$R_{d\text{-}WE}$	286.9 Ω	649.7 Ω	1597 Ω	1032 Ω
$R_{d\text{-}bulk}$	22.21 Ω	21.56 Ω	22.43 Ω	17.15 Ω

Table S3. Tabulated photovoltaic parameters of DSCs employing T+Z1 photoanodes with different ZnO layer thicknesses (5µm, 15µm and 25µm), sensitized with Y123 dye, and $[Cu(dmp)_2]^{1+/2+}$ redox electrolyte under AM 1.5G (100 mW/cm²) irradiation.

ZnO layer thickness (µm)	V_{OC} [a] (V)	J_{SC} [a] ($mAcm^{-2}$)	FF [a]	PCE [a] (%)
5	1.11 (1.11)	9.66 (9.65)	0.66 (0.67)	7.12 (7.10)
15	1.13 (1.13)	10.06 (10.07)	0.66 (0.66)	7.54 (7.49)
25	1.12 (1.12)	9.79 (9.82)	0.68 (0.67)	7.42 (7.38)

[a] J-V parameters of champion cells and averages taken over five sets of samples (in parentheses) with a maximum mean deviation of ± 0.01, ± 0.10, ± 0.02 and ± 0.05 in V_{OC}, J_{SC}, FF and PCE, respectively.

Table S4. Photovoltaic parameters of the DSCs employing T+Z1+BL photoanodes sensitized with MS5 dye and $[Cu(dmp)_2]^{1+/2+}$ redox electrolyte under standard 1000 lux CFL and LED illuminations.

Illumination source	Intensity	P_{in} ($\mu W/cm^2$)	V_{OC} [a] (V)	J_{SC} [a] (μAcm^{-2})	FF [a]	PCE [a] (%)	P_{max} [a] ($\mu W/cm^2$)
CFL	**1000 lux**	**283**	1.025 (1.014)	37.14 (37.44)	0.82 (0.81)	11.07 (10.94)	31.33 (30.97)
LED	**1000 lux**	**313**	1.025 (1.013)	38.20 (39.17)	0.82 (0.81)	10.31 (10.24)	32.28 (32.08)

[a] J-V parameters of champion cells and averages taken over five sets of samples (in parentheses) with a maximum mean deviation of ± 0.015, ± 1.44, ± 0.02, ± 0.18 and ± 0.50 in V_{OC}, J_{SC}, FF, PCE and P_{max} respectively.

Illumination source & intensity	Year	Best reported V_{OC} (V)	Reference
	2017	1.10	[3]
	2018	1.14	[4]

Table S5. Highest V_{OC} values reported in literature using dyes and organic copper for DSCs electrolyte (since 2017) under outdoor and indoor illuminations.

	2019	1.10	[5]
	2020	1.08	[6]
	2021	1.24	[7]
	2022	1.22	[8]
	2023	**1.27**	**Present work**
fluorescent light (1000 lux)	2017	0.80	[3]
	2018	0.88	[9]
	2019	0.94	[5]
	2020	0.91	[6]
	2021	0.98	[7]
	2022	0.92	[10]
	2023	**1.025**	**Present work**
LED light (1000 lux)	2022	1.02	[8]
	2023	**1.025**	**Present work**
High power LED light (200 mW/cm^2)	**2023**	**1.295**	**Present work**

REFERENCES

1 S. Sasidharan, A. Jagadeesh, S. C. Pradhan, B. N. Nair, A. Azeez Peer Mohamed, K. N. Narayanan Unni, S. Soman and U. Nair Saraswathy Hareesh, *Solar Energy*, 2021, **226**, 214–224.

2 F. S. Husairi, S. M. Ali, A. Azlinda, M. Rusop and S. Abdullah, *J Nanomater*, 2013, **2013**, 148.

3 M. Freitag, J. Teuscher, Y. Saygili, X. Zhang, F. Giordano, P. Liska, J. Hua, S. M. Zakeeruddin, J. E. Moser, M. Grätzel and A. Hagfeldt, *Nature Photonics 2017 11:6*, 2017, **11**, 372–378.

4 Y. Saygili, M. Stojanovic, H. Michaels, J. Tiepelt, J. Teuscher, A. Massaro, M. Pavone, F. Giordano, S. M. Zakeeruddin, G. Boschloo, J. E. Moser, M. Grätzel, A. B. Muñoz-García, A. Hagfeldt and M. Freitag, *ACS Appl Energy Mater*, 2018, **1**, 4950–4962.

5 P. Ferdowsi, Y. Saygili, F. Jazaeri, T. Edvinsson, J. Mokhtari, S. M. Zakeeruddin, Y. Liu, M. Grätzel and A. Hagfeldt, *ChemSusChem*, 2020, **13**, 212–220.

6 H. Michaels, M. Rinderle, R. Freitag, I. Benesperi, T. Edvinsson, R. Socher, A. Gagliardi and M. Freitag, *Chem Sci*, 2020, **11**, 2895–2906.

7 D. Zhang, M. Stojanovic, Y. Ren, Y. Cao, F. T. Eickemeyer, E. Socie, N. Vlachopoulos, J. E. Moser, S. M. Zakeeruddin, A. Hagfeldt and M. Grätzel, *Nat Commun*, 2021, **12**, 1777.

8 Y. Ren, D. Zhang, J. Suo, Y. Cao, F. T. Eickemeyer, N. Vlachopoulos, S. M. Zakeeruddin, A. Hagfeldt and M. Grätzel, *Nature*, 2023, **613**, 60–65.

9 Y. Cao, Y. Liu, S. M. Zakeeruddin, A. Hagfeldt and M. Grätzel, *Joule*, 2018, **2**, 1108–1117.

10 C. C. Chen, V. S. Nguyen, H. C. Chiu, Y. Da Chen, T. C. Wei and C. Y. Yeh, *Adv Energy Mater*, 2022, **12**, 2104051.